

Correlation between photoluminescence and ellipsometric measurements of porous silicon layers

S. RAHMOUNI^{a,b,*}, L. ZIGHED^c, S. CHAGUETMI^d, M. DAOUDI^e, M. KHELIFA^f, M. KARYAOUF^g, R. CHTOUROU^g

^aDepartment of Electrical Engineering, 20 Aout 1955 University of Skikda, Algeria

^bNormal Higher School of Technological Education, (ENSET) Skikda, Algeria

^cLaboratory of Chemical and Environmental Engineering, 20 Aout 1955 University of Skikda, Algeria

^dLaboratory of LSPN, 08 Mai 1945 University of Guelma, Algeria

^eLaboratory of Energetic Research and Material Developments for nuclear Sciences, National centre of Nuclear Science and Technology, 2020 Sidi-Thabet, Tunisia

^fSemiconductor and Advanced Technology, Laboratory of Nanostructured. Centre of Research and Energetic Technology, Techno-Park Borj-Cedria, B.P.N° 95, Hammam-Lif, 2050 Tunisia

^gLaboratory for nanomaterials and systems for renewable energies (LANSER), Techno-Park Borj-Cedria, B.P.N° 95, Hammam-Lif, 2050 Tunisia

Herein, we studied the linked physical proprieties between the photoluminescence and the ellipsometric measurements of porous silicon layers. Porous silicon layers were elaborated by the electrochemical etching method, using doped *p*-type (100)-oriented silicon substrate. The photoluminescence (PL) and the spectroscopic ellipsometry (SE) measurements were used to study the porous silicon layers that obtained from different etching current density and etching time. In order to apply the ellipsometry measurements, we needed to make a model of multi-layer structures that allow us to figure out the thickness and porosity of each layer. Our results showed that at some current density and some time, the porous silicon layer was etched. Additionally, we amusingly noticed a significant improvement in luminescence intensity. The study confirmed a real correlation between photoluminescence and ellipsometric measurements of porous silicon layers.

(Received September 5, 2017; accepted October 10, 2018)

Keywords: Porous silicon, Antireflective coating, Electrochemical anodization, Photoluminescence, Spectroscopic ellipsometry

1. Introduction

In previous years, porous silicon is rapidly attracting increasing interest in various fields and has received a great deal of attention from researchers because of its potential use in a variety of industrial applications such as photovoltaic device applications [1–4], chemical and gas sensors [5–12], biosensors [13,14], and biomedical applications [15], micromachining [16-18], templates for micro- and nanofabrication [19–21] solar cells and photoluminescence [1,22,23]. However, a very limited data of optoelectronic uses in this field are available [24,25]. It's reported that the photoluminescence of porous silicon (PS) has achieved a large-scale investigation, giving an explanation of the photoluminescence phenomenon by getting the optical proprieties of porous silicon, along with the focus on the determination of its refractive index and the gap energy, that can be determined whether by direct measurement of absorption or by a non-destructive technique called spectroscopic ellipsometry (SE).

However, the physical and optical properties could be studied. In addition, some of the physical phenomena are still poorly understood because of the strong relationship

between the pSi nanostructure and the elaboration conditions, (HF concentration, current density, and anodization time) [26]. The present study conclusively suggested that in order to prepare porous silicon samples, we need to determine the optimal conditions that lead to increase the optical efficiency. Herein, we need to study the correlation between the results extracted from the PL analysis and those obtained by ellipsometry. The study of the evolution of the intensities of the emission spectra obtained by the measurement PL as a function of the porosity and the thickness determined by ellipsometry of the layers, for silicon substrates oriented P- 100 of low resistivity is made to precisely clarify the evolution of optical parameters.

2. Expérimental details

Serial of porous silicon samples were prepared of *p*-type (100)-oriented silicon substrate with a resistivity of 0.001–0.02 Ω cm. The electrochemical cell was made of Teflon, while the base plate was made of aluminum. A silicon wafer was mounted at the base plate, making an *o*-ring of Si surface of 0.64 cm², which was exposed to the electrolytes. The porous silicon layers were performed

using a computer interface controlled electrochemical etching method by a mixture solution of hydrofluoric acid HF (40%) C₂H₅OH (98%) (1:1) volume ratio. The Si wafers were ultrasonically cleaned in ethanol, acetone and then dried by nitrogen, before starting of each experiment.

The PL measurements were carried out by a solid laser 447 nm, and detected through a Jobin Yvon 250 mm HR mono-chromator, with a GaAs photomultiplier associated to standard lock-in technique. Of note, the laser power of 7.66 mW was applied on the surface of the sample. A Ge5 Sopra made rotating polarizer spectroscopic ellipsometer was used for the (SE) spectroscopic ellipsometry measurement.

3. Results and discussion

All of the PS samples showed a visible PL at a room temperature. The Fig. 1 illustrates the PL spectra of samples of p-type elaborated at different etching time (60, 120, 180 and 240 seconds), as well as an etching current density of 15 mA/cm².

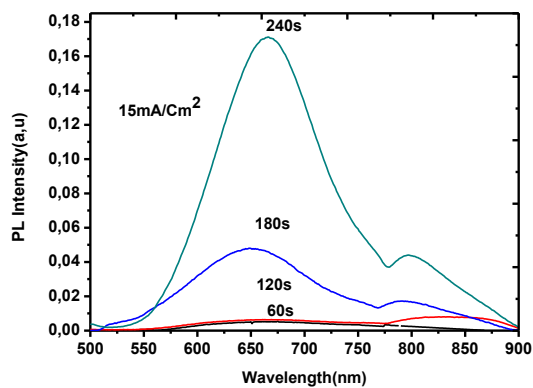


Fig. 1. Evolution of photoluminescence spectra of P-type porous silicon prepared at different etching time

The Fig. 1 shows that the observed large band that ranges from 550 nm and 780 nm, decreases in time with a peak of 668 nm, and a decreased full width at half maximum (FWHM) from 226 to 112, along with an increase of PL intensity from 0,07 to 21,06.

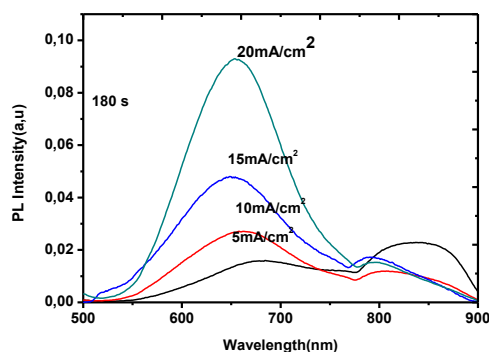


Fig. 2. Evolution of photoluminescence spectra of P-type porous layers prepared at different etching current density

The Fig. 2 shows the PL spectra of p-type samples that were obtained from different etching current density 5, 10, 15 and 20 mA / cm², and etching time of 180s. The presented serial in Fig. 1 indicates near similar variations of the PL intensity. However, a remarkable increase of the PL intensity ranges from 2, 59 to 11, 72 was noticed.

The two spectra show an improvement in the PL intensity as a function of etching current density and etching time. On the other hand, we noticed that the PL intensity reached the maximum value of J_{CM}, that equals 20mA / cm², with t_m = 240sec. The slight blue-shift energy of PL band allow us to attribute a confinement of more and more wells and wire that leads to diminution of nano-crystallite size [27, 28].

The porous layer obtained from p-type silicon wafer is presented as cylindrical and spherical crystallites [29, 30]. Therefore, PSi is defined as a mixture of quantum wells (QW), and quantum wire following different concentrations and sizes. In the case of the increased etching time, the thickness of porous silicon layer increases from 106.3 nm to 1027.2 nm (Table 3).

The proprieties of PS porous silicon Depends on the anodisation conditions. The thickness and the porosity, respectively Depends on the etching time and the applied current density. To extract the thickness of the PS layer from measuring of SE, an optical model must be assumed, as well as the calculated data have to follow experimental spectra. In applying EMA software, we utilized a model of a multi-layer model, whereas the first mixture of the layer (void/SiO₂), while the second layer is (SiCr/void), As indicated in Fig. 3 a high improvement in the fit quality was observed.

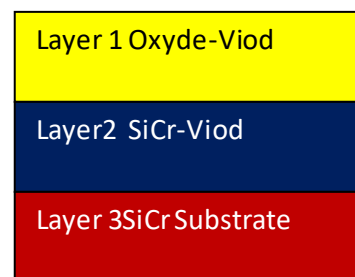


Fig. 3. The multilayer model of the PSL

Also, the ellipsometry spectroscopy measurement show that the increase in the current anodisation density leads to an increase in porosity of the porous layers from 34.53% to 78.23%. PL parameters are summarized in Table 1 and 2. According to the previous results, the correlation is studied between the PL and SE measurements.

Table 1. Optimized fitting parameters corresponding to the theoretical curves, of porous silicon samples prepared at different etching time and current density of 15mA/cm²

Samples	Etching Time (s)	λ_{Pic} (nm)	FWHM (meV)	I_{PLMax} (u,a)	E_g (eV)
S1	60	628	226	0.07	1.96
S2	120	666	189	0.89	1.86
S3	180	652	122	6.81	1.91
S4	240	668	112	21.06	1.86

Table 2. Optimized fitting parameters corresponding to the theoretical curves, of porous silicon samples prepared at different etching current density and etching time of 180s

Samples	Current Density (mA/Cm ²)	λ_{Peak} (nm)	FWHM (meV)	I_{PLMax} (u,a)	E_g (eV)
S5	5	682	249	2.59	1.81
S6	10	665	210	4.12	1.87
S7	15	652	122	6.81	1.91
S8	20	655	111.	11.72	1.90

Table 3. Different parameters evaluated from the optical model of samples obtained at different etching time, and different current density

Samples	Etching Time (s)	Current Density (mA/Cm ²)	Thickness (μ m) (d)	Porosity(%) (P)	n	k
S1	60	15	0.1063	36.02	/	/
S2	120	15	0.7061	58.84	/	/
S3	180	15	0.9058	70.20	/	/
S4	240	15	1.0272	76.89	/	/
S5	180	5	0.0985	34.53	1.77	0.0035
S6	180	10	0.7221	61.45	1.43	0.0022
S7	180	15	0.9058	70.20	1.33	0.0018
S8	180	20	1.0311	78.23	1.22	0.0014

The Fig. 4 depicts that the thickness and the integral intensity of the PL increase as function of etching time, meanwhile the porosity and the integral intensity of PL increase as a function of the current density (Fig. 5). On the other hand, the PL intensity of the porous layer increases as a function of etching time and current density.

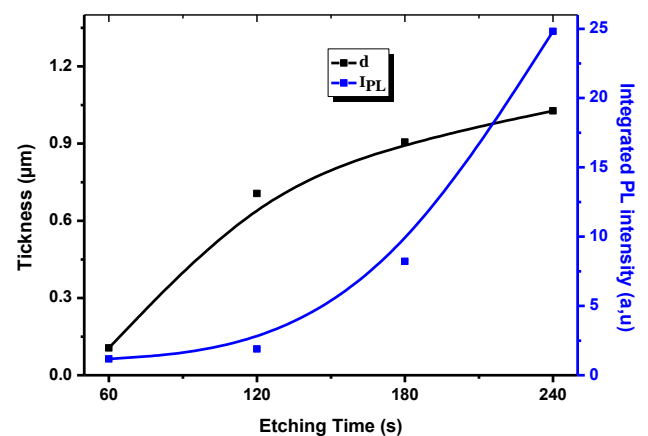


Fig. 4. Variation of thickness and integrated PL intensity according to etching time

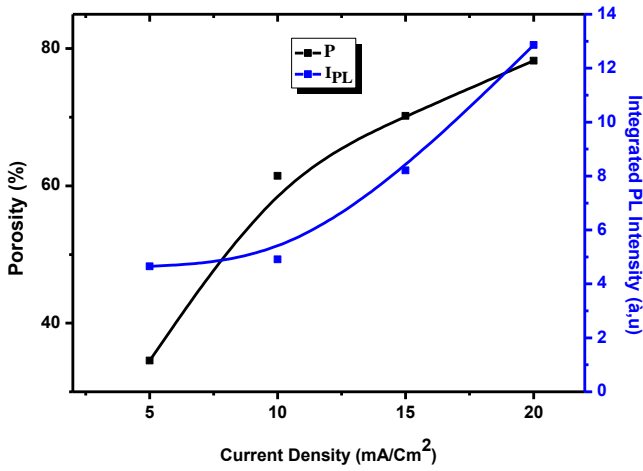


Fig. 5. Variation of porosity and integrated PL intensity according to etching current

The first serial of samples obtained from a current density of 15mA/cm² and etching time varying from 60 to 240 seconds.

The measure and the shape of the ellipsometrical spectra are presented in Figs. 6 and 7.

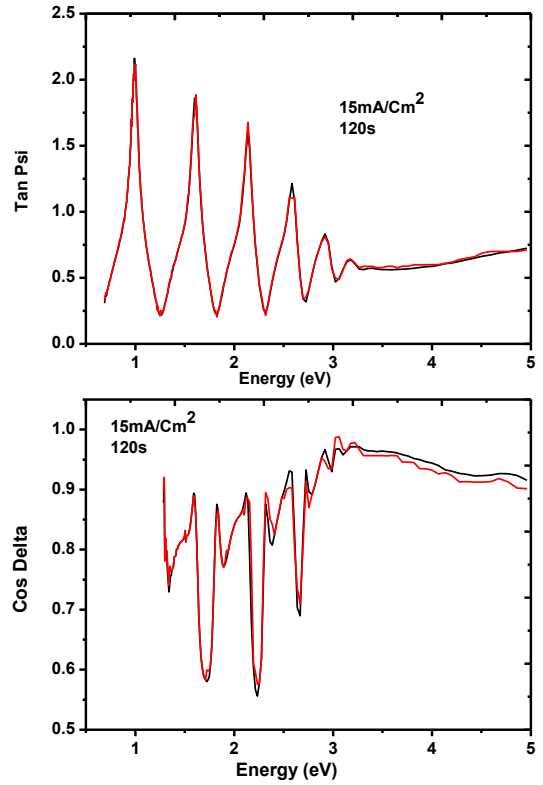


Fig. 7. SE measurements of the PSL obtained in using 15mA/cm², 180s and the calculated spectra based on the best fitted parameters

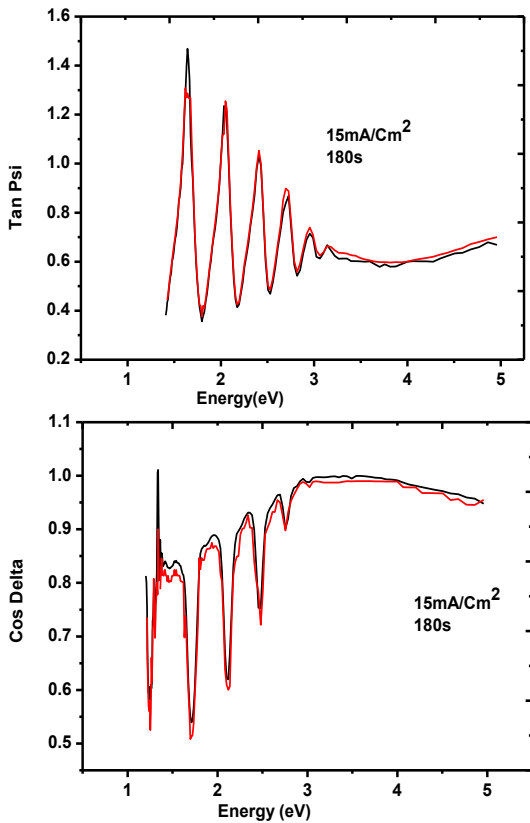


Fig. 6. SE measurements of the PSL obtained in using 15mA/cm², 120s and the calculated spectra based on the best fitted arameters

The first serial allows us to determine ellipsometry. The adjustment parameters for the thickness of separated layers, using each sub-layer of the optical model are summarized in Table 3. The second serial of samples was obtained following an etching time of 180s and a current density varying from 5mA/cm² to 20 mA/cm². The Fig. 8 and 9 show the measurement and the shape of ellipsometry spectra.

The second serial allows us to determine the porosity of separated layers, using ellipsometrical method. The adjustment parameters for each sub-layer of an optical model are summarized in Table 3.

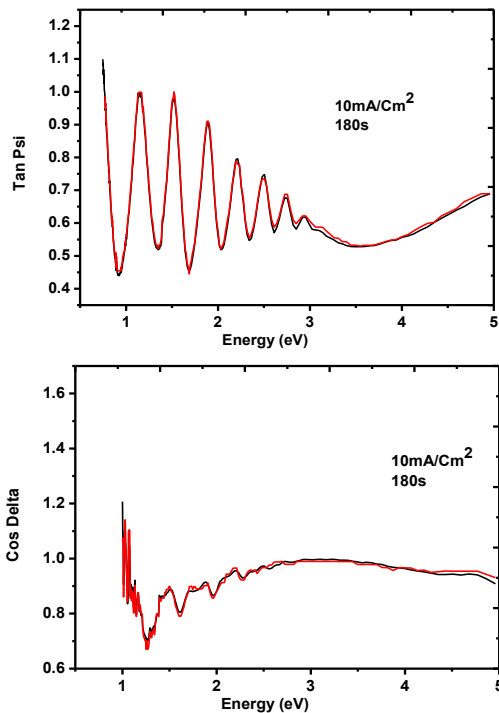


Fig. 8. SE measurements of the PSL obtained in using $5\text{mA}/\text{cm}^2$, 180s and the calculated spectra based on the best fitted parameters

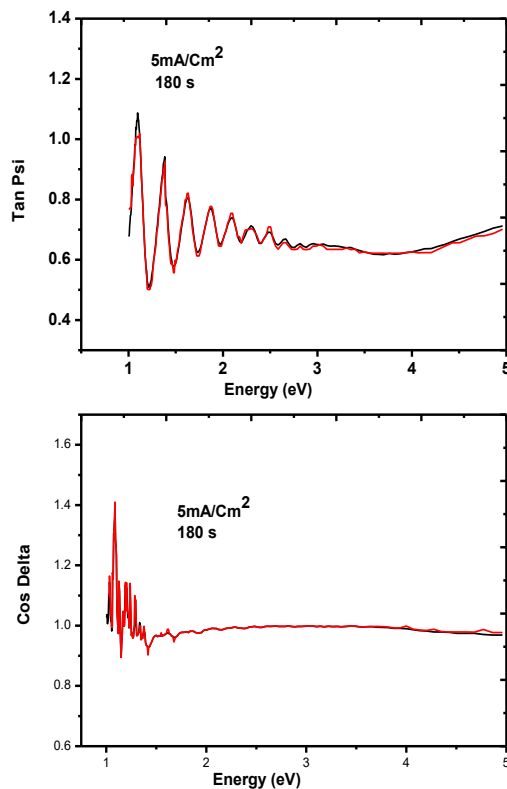


Fig. 9. SE measurements of the PSL obtained in using $10\text{mA}/\text{cm}^2$, 180s and the calculated spectra based on the best fitted parameters

The Fig. 4 shows an agreement between the PL measurement presented by the integral intensity of PL, along with the SE measurement presented by the thickness of porous layers obtained through varying etching time. In parallel,

The Fig. 5 shows an agreement between the PL measurement presented by integral intensity of PL and SE measurement presented by the porosity of porous layers obtained following varying current density.

The two produced curves using values obtained by ellipsometry show that the thickness is as an increased function following etching time; meanwhile the porosity is as an increased function following the current density [31].

In this case, the PL comportment can be explained by the absence of the laser interference in the cleaned layer, as previously indicated. The contrary case was noticed in the thickness and the porous layer of silicon variations.

The measurement of the refractive index (n), the extinction coefficient (k) and the porosity (p) of porous layers by ellipsometry present an obvious correlation between the measurements by PL and those by SE. The results illustrated in Table 3 and Fig. 10 show that the refractive index and the extinction coefficient are as a decreased function along with the porosity.

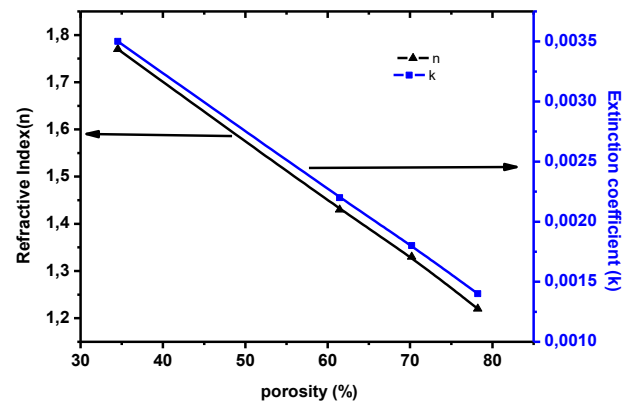


Fig. 10. Variation of refractive index and extinction coefficient as a function of porosity

In case of a porosity of 34%, we get $n = 1,77$ and $k = 0,0035$, while for porosity of 78%, we get $n = 1.22$ and $k = 0,0014$.

This result shows that the remained porous layer is more proper, but less thick and gives us a best PL intensity. Hence, the laser diffuses in wells by confinement effect, This confinement means to confine the incident laser radiation in crystallites seals, and therefore the laser reflection is reduced following the big values of thickness and the porous layers.

4. Conclusion

In this study, we developed porous silicon layers by electrochemical anodization, the optical characterization made by spectroscopic ellipsometry (SE) and photoluminescence (PL), this characterization enabled us to calculate the physical and optical parameters (porosity, thickness) (refractive index and extinction coefficient). To determine the effect of the etching parameters, we have suggested that for a good elaboration of the porous layers, it would be necessary to know the optimal conditions of anodization taking into account the great role of the oxide layer on the surface. we note that The results obtained demonstrate that it excites a correlation between photoluminescence characterization (PL) and measurement of spectroscopic ellipsometry (SE), this results is very important in the photovoltaic field.

References

- [1] A. Ramirez, W. J. Aziz, Z. Hassan, K. Omar, K. Ibrahim, *Optik- Int. J. for Light and Elect. Optics* **122**(23), 2075 (2011).
- [2] B. A. Mohamed, H. Anouar, B. Brahim, *Sol. Energy*. **86**(5), 1411 (2012).
- [3] S. Sanchez de la Morena, G. Recio-Sanchez, V. Torres-Costa, R. J. Martin-Palma, *Scripta Mater.* **74**, 33 (2014).
- [4] M. Atyaoui, W. Dimassi, A. Atyaoui, J. Elyagoubi, R. Ouertani, H. Ezzaouia, *J. Lumin.* **141**, 1 (2013).
- [5] F. A. Harraz, A. A. Ismail, H. Bouzid, S. A. Al-Sayari, A. Al-Hajry, M. S. Al-Assiri, *Appl. Surf. Sci.* **307** (2014).
- [6] A. Bardaoui, R. Chtourou, M. Amlouk, *Nova Science Publishers* (2012).
- [7] M. S. Salem, M. J. Sailor, F. A. Harraz, T. Sakka, Y. H. Ogata, *J. Appl. Phys.* **100**(8), 083520 (2006).
- [8] T. V. K. Karthik, L. Martinez, V. Agarwal, *Journal of Alloys and Compounds* **731**, 853 (2018).
- [9] M. S. Salem, M. J. Sailor, F. A. Harraz, I. Sakka, Y. H. Ogata, *Phy. Stat. Sol. C* **4**(6), 2073 (2007).
- [10] M. Li, M. Hu, P. Zeng, S. Ma, W. Yan, Y. Qin, *Electrochem. Acta* **108**, 167 (2013).
- [11] P. Dwivedi, Das, S. Dhanekar, *ACS Appl. Mater. Interfaces* **9**(24), 21017 (2017).
- [12] F. A. Harraz, A. A. Ismail, H. Bouzid, S. A. Al-Sayari, A. Al-Hajry, M. S. Al-Assiri, *Int. J. Electrochem. Sci.* **9**, 2149 (2014).
- [13] V. Myndrul, R. Viter, M. Savchuk, N. Shpyrka, D. Erts, D. Jevdokimovs, V. Silamiķelis, V. Smyntyna, A. Ramanavicius, I. Iatsunskyi, *Biosensors and Bioelectronics* **102**, 661 (2018).
- [14] F. A. Harrez, *Sensors and Actuat. B. Chem.* **202**, 897 (2014).
- [15] T. Sarkar, D. Basu, N. Mukherjee, Ja. Das, *Materials Today Science Direct* **5**(3) Part 3, 9798 (2018).
- [16] X. Sun, G. Parish, A. Keating, *Sensors and Actuat. A: Physical* **269**, 91 (2018).
- [17] Ryan A. Wallace, Michael J. Sepaniak, Nickolay V. Lavrik, Panos G. Datskos, *Anal. Chem.* **89**(11), 6272 (2017).
- [18] V. Lysenko, S. Perichon, B. Remaki, D. Barbier, *Sensors and Actuators A* **99**, 13 (2002).
- [19] Ch. Jia, S. He, J. Song, Y. Jin, W. Zhu, Q. Cheng, *Cellulose Chem. Technol.* **51**(7-8), 693 (2017).
- [20] H. V. Bandarenka, V. Girel, S. A. Zavatski, A. Panarin, S. N. Terekhov, *Materials* **11**(5), 852 (2018).
- [21] F. A. Harraz, *Phys. Stat. Solid C* **8**(6), 1883 (2011).
- [22] A. S. Lenshin, P. V. Seredin, V. M. Kashkarov, D. A. Minakov, *Materials Science in Semiconductor Processing* **64**, 71 (2017).
- [23] K. Omar, K. A. Salman, *Journal of Nano Research* **46**, 45 (2017).
- [24] C. Mazzdeni, L. Pavesi, *Appl. Phys. Lett.* **67**(20), 2983 (1995).
- [25] H. A. Hadi, R. A. Ismail, N. F. Habubi, *Indian Journal of Physics* **88**(1), 59 (2014).
- [26] Jian-Ming Ji, Xiu-Xia He, Qian Duan, Zhen-Xin Wang, *Chin. J. Anal. Chem.* **41**(5), 698 (2013).
- [27] D. T. J. Ee, C. K. Sheng, *The Malaysian J. Anal. Sci.* **15**(2), 227 (2011).
- [28] B. Gelloz, *Appl. Surf. Sci.* **108**(4), 449 (1997).
- [29] A. G. Cullis, L. T. Canham, O. D. Dossor, *Mater. Res. Soc. Symp.* **256**(7), (1992).
- [30] I. Berbezier, A. Halimaoui, *J. Appl. Physics* **74**(9), 5421 (1993).
- [31] S. Rahmouni, L. Zighed, I. Tifouti, S. Hadnine, M. S. Aida, *Optoelectron. Adv. Mat.* **11**(1-2), 105 (2017).

^{*}Corresponding author: rahmouni.eln@gmail.com